PHYSICAL REVIEW B VOLUME 6, NUMBER 5 1 SEPTEMBER 1972

Neutron-Scattering Study of Spin Waves in the Ferrimagnet $RbNiF_3$

J. Als-Nielsen
Danish A.E.C. Research Establishment Risö, Roskilde, Denmark

and

R. J. Birgeneau
Bell Laboratories, Murray Hill, New Jersey 07974
and Danish A.E.C. Research Establishment Risö, Roskilde, Denmark

and

H. J. Guggenheim
Bell Laboratories, Murray Hill, New Jersey 07974
(Received 29 February 1972)

$RbNiF_3$ is a transparent hexagonal ferrimagnet with $T_c = 133$ °K. Below T_c the Ni^{++} magnetic moments are aligned collinearly in ferromagnetic hexagonal sheets with a stacking sequence of these planes *BBABBA* such that the *A* spins are antiparallel to the *B* spins. This magnetic structure is determined by a 180° antiferromagnetic exchange between nearest-neighbor *A*, *B* spins and a 90° ferromagnetic exchange between nearest-neighbor *B* spins. In this paper we report a detailed inelastic-neutron-scattering study of the spin waves in $RbNiF_3$ both at low temperatures and through T_c. The magnetic unit cell contains six Ni^{++} spins so that there are in general six distinct branches in the spin-wave spectrum. All six branches are observed in the ΓA direction (*c* axis), while only the lowest three are observed in the ΓM direction. The measured dispersion curves at 4.2 °K may be accurately fitted using simple spin-wave theory with $J_{AB} = (93.2 \pm 2)$ °K, $J_{BB} = -(21.1 \pm 2)$ °K ($\mathcal{H} = \sum_{i>j} J_{ij} \vec{S}_i \cdot \vec{S}_j$, $S = 1$), and with all other exchange constants set to zero. Using these exchange constants we can satisfactorily account for other magnetic properties such as the high-temperature susceptibility, the sublattice magnetizations in a field, and two-magnon Raman scattering. At higher temperatures it is found that the *c*-axis acoustic magnons renormalize like the magnetization, whereas the high-lying optic modes are nearly temperature independent. This leads one to the physical picture in which $RbNiF_3$ at high temperatures is viewed as a set of strongly correlated two-dimensional ferrimagnets composed of three successive planes *BAB* coupled by the strong exchange field $H_{AB} \sim 6J_{AB}$; these *BAB* "two-dimensional ferrimagnets" are then coupled together by the much weaker exchange field $H_{BB} \sim J_{BB}$.

I. INTRODUCTION

In the past decade detailed experimental and theoretical investigations of the spin-wave dispersion relations and the concomitant thermodynamic properties have been carried out in a large number of localized antiferromagnets.[1-5] Neutron-scattering experiments have also been performed in certain localized ferromagnets such as $CrBr_3$,[6] EuO, and EuS,[7] although the number of these has been rather limited because of the paucity of suitable systems. On the other hand, rather little information is available on the excitations in *ferrimagnets* in spite of the abundance of such systems. Indeed, the only ferrimagnet whose dispersion relations have been examined in any detail is Fe_3O_4, due to the pioneering neutron-scattering work of Riste[8] and Brockhouse and Watanabe.[9] It is therefore of considerable interest to apply inelastic-neutron-scattering techniques to other ferrimagnets both as a test of spin-wave theory and to elucidate their microscopic magnetic behavior. Indeed, as we shall see, in even moderately complicated systems direct measurement of the dispersion relations is often the only method of obtaining unambiguous values for the exchange constants.

A ferrimagnet which is both relatively simple and of some current interest is the compound $RbNiF_3$. It is a transparent hexagonal ferrimagnet[10] with a transition temperature of 133 °K.[11,12] The unit cell contains six essentially identical spins, four parallel and two antiparallel,[13] so that in general there are six branches in the spin-wave spectrum. In the *c* direction these reduce to three in a double-zone scheme; this is, in fact, the simplest possible spectrum in a collinear ferrimagnet made up of identical spins. To date, experimental work in $RbNiF_3$ has been reported on the crystallographic[10,14] and magnetic structure,[13] magnetic resonance,[15] magnetization and susceptibility,[11,12] Faraday rotation,[16] nuclear resonance,[16,17] optical spectroscopy,[18,19] and two-magnon Raman scattering.[20-22] However, it has not been possible to extract unambiguous interaction parameters from these experiments. Recently, a detailed the-

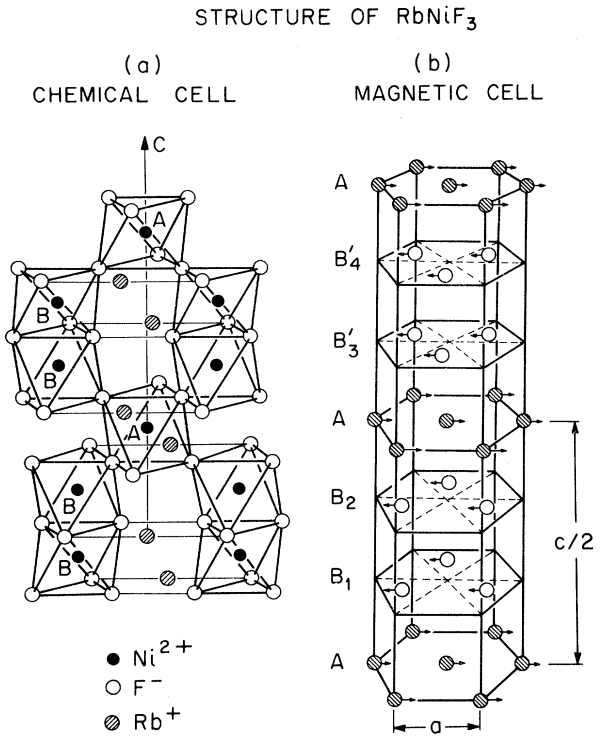

FIG. 1. (a) Structure of $RbNiF_3$. The Ni ions are located in the center of fluorine octahedra, which share faces (at B sites) or corners (at A sites) with adjacent octahedra. (b) Magnetic structure in $RbNiF_3$. The spins lie in layers of hexagonal symmetry with the stacking sequence $ABBAB'B'A\ldots$.

oretical investigation of $RbNiF_3$ has been carried out by Chinn, Zeiger, and O'Connor.[22] These authors have given a complete theory for the spin-wave dispersion relations. In addition, using exchange parameters estimated from the magnon-sideband experiments of Zanmarchi and Bongers,[18] they have calculated various magnetic properties such as T_c, the sublattice magnetizations in an applied field, and the two-magnon Raman scattering.

Stimulated both by the wealth of preexisting experimental information and the theoretical work of Chinn *et al.*,[22] we have carried out a detailed neutron-scattering investigation of the spin-wave dispersion relations in $RbNiF_3$ both at 4.2 °K and as a function of temperature through T_c. In this paper we report these measurements and an analysis of them using the theory of Chinn *et al.* Our exchange constants differ substantially from the estimates of Chinn *et al.* and the spin-wave spectrum is correspondingly very different from theirs. Using the exchange constants from our neutron-scattering experiment, we shall discuss other magnetic properties such as θ, T_c, etc. We shall also discuss the two-magnon Raman scattering, which is particularly interesting in this material.

Finally, it should be noted that $RbNiF_3$ offers the unusual opportunity of measuring both 90° and 180° exchange constants simultaneously in a fluoride lattice. These are of considerable interest for superexchange calculations.[23,24] As we shall see, the results are found to be consistent with overlap considerations and with the exchange found in other systems such as $KNiF_3$[22] and K_2NiF_4.[4]

The format of the paper is as follows: In Sec. II we discuss the sample preparation and the crystal and magnetic structure. In Sec. III the spin-wave theory will be reviewed. Section IV contains details of the experiment including the technique, results, and simple spin-wave analysis. In Sec. V these results are discussed and comparisons with other experiments will be made. Finally, the conclusions are given in Sec. VI.

II. CRYSTAL STRUCTURE AND SAMPLE PREPARATION

Single crystals of $RbNiF_3$ may be readily grown using standard techniques. RbF was first zone refined into large single crystals. Polycrystalline NiF_2 was prepared from high-purity Ni-metal sponge. The RbF and NiF_2 were then loaded into a platinum crucible quantitatively in the ratio 1:1. A Bridgman technique, which has been described previously,[25] was then used to grow the crystal. Because the compound $RbNiF_3$ is congruently melting, this method can produce good single crystals. The actual crystal used in this experiment had a volume of 10 cm^3 and was approximately elliptical in shape with an aspect ratio of 2:1. The mosaic spread was ~1° full width at half-maximum.

The crystal structure of $RbNiF_3$ is illustrated in Fig. 1. The crystal is hexagonal, space group D^4_{6h} ($P6_3/mmc$) with a configuration like that of the hexagonal modification of $BaTiO_3$. A detailed crystal-structure analysis has been reported by Weidenborner and Bednowitz,[14] who give precise values for all of the appropriate bond lengths and bond angles. The room-temperature lattice constants of the unit cell, which contains six formula units, are $a = 5.840 \pm 0.002$ Å and $c = 14.308 \pm 0.004$ Å. All of the ions in this structure occupy special positions. The nickel ions occupy two nonequivalent sites, labeled A and B in Fig. 1, at the center of fluorine octahedra. Two-thirds of the NiF_6 octahedra, that is, those containing Ni(B) ions, occur in face-sharing pairs to form Ni_2F_9 polyhedra. The remaining NiF_6 octahedra are linked to the Ni_2F_9 polyhedra by sharing of corners. The Ni(B)-Ni(B) and Ni(A)-Ni(B) distances together with the appropriate fluorine bond angles are given in Table I. The Ni(A)-Ni(B) distance is quite close to that found for nearest neighbors in $KNiF_3$ and K_2NiF_4 and the bond angle is close to 180°. The Ni(B)-Ni(B) ions form pairs with a fluorine superexchange bond angle close to 90°. We shall discuss the con-

TABLE I. Experimental values for Ni^{++}-Ni^{++} exchange in fluorides and oxides with octahedral coordination.

Material	Ni^{++}-Ni^{++} Distance[a](Å)	$F^-(O^{--})$ Bond angle	Direction	J[f] (°K)
K_2NiF_4[b]	4.006	180°	[100]	112.3±0.4
$KNiF_3$[c]	4.014	180°	[100]	102.2±1.2
$RbNiF_3$	4.034	178.2°	[100]	93.2±2
	2.728	84.1°	[111]	−21.1±2
NiF_2[d]	3.084	100.2°	[110]	−0.2
NiO[e]	4.172	180°	[100]	221±4
	2.950	90°	[110]	−16±10

[a]Room-temperature value.

[b]Reference 4.

[c]Reference 22.

[d]M. T. Hutchings, M. F. Thorpe, R. J. Birgeneau, P. A. Fleury, and H. J. Guggenheim, Phys. Rev. B 2, 1362 (1970).

[e]Reference 5.

[f]It should be noted that all of these exchange constants have been deduced from simple spin-wave theory and thus they may be shifted by ~5% by higher-order Oguchi-type corrections.

sequences of these two configurations for the superexchange in Sec. III. The nickel positions alone are illustrated in Fig. 1(b). The nickel atoms form hexagonal sheets with a stacking sequence $BBAB'B'A$.

As noted in Sec. I, $RbNiF_3$ orders ferrimagnetically at 133 °K. This ferrimagnetism was discovered independently by Smolenskii *et al.*[11] and Schafer *et al.*[12] and investigated thoroughly by both groups. They have proposed that the magnetic structure is such that the Ni^{++} spins lie in the basal plane with the B spins parallel and A spins antiparallel. This necessitates that the magnetic and chemical unit cells coincide. Recently this proposed structure has been confirmed directly by neutron scattering by Pickart and Alperin.[13] Our own elastic-scattering measurements, which were limited in extent, are also consistent with this structure. T_c (133 °K) was determined both from measurements of the sublattice magnetization and from observations of the peak in the wave-vector-dependent susceptibility near a reciprocal-lattice point. T_c in our crystal is somewhat lower than typical values previously reported (138–145 °K).

III. SPIN-WAVE THEORY

The spins of the Ni^{++} ions are coupled mainly by superexchange via the intervening F^- ions. As shown in Fig. 1(a) and noted in Sec. II, each Ni^{++} ion is located in the center of an octahedron of F^- ions. Thus only spins in adjacent layers along the c axis can couple in a superexchange path involving one F^- ion only. The dominant interactions are therefore J_{BB} between nearest-neighbor B atoms and J_{AB} between B and A atoms. The B atoms share a face of their octahedron, whereas a B atom and an A atom share a corner. The angle in the superexchange path is thus approximately 90° for a B-B path and 180° for a B-A path. From Anderson's theory[23] of superexchange and also by analogy with NiO, where there is also both 90° and 180° exchange,[5] we expect J_{AB} to be strong and antiferromagnetic, whereas J_{BB} should be ferromagnetic and probably somewhat weaker. The magnetic structure is of course consistent with this expectation, and the dynamics of the spin system will directly reflect the strength of the ferromagnetic and antiferromagnetic coupling. Before we analyze these magnon-dispersion relations, it is convenient first to consider the effective anisotropy as well as coupling to more distant neighbors.

The anisotropy field in this case is such that the spins lie in the plane perpendicular to the c axis. Schafer *et al.*[12] find that a field of only 30 kG is necessary to align the spins along the c axis; the corresponding energy per spin is small compared to the exchange energies. The in-plane anisotropy is significantly smaller than this uniaxial anisotropy. Magnetic-resonance studies of $RbNiF_3$ at 77 °K have been reported by Golovenchits *et al.*[15] They find a single mode whose resonance frequency extrapolates to zero with zero applied field. Thus the spin waves must have zero gap. From the dependence of the resonance field on direction, they deduce that the out-of-plane anisotropy field is given by $g\mu_B H_A = 0.25$ meV. This is two orders of magnitude smaller than the observed exchange fields. Thus we may safely neglect any anisotropy terms in the spin Hamiltonian. To estimate further-neighbor interactions we compare $RbNiF_3$ with K_2NiF_4, in which the nearest-neighbor 180° superexchange is 112 °K. In K_2NiF_4 the second-neighbor interaction which involves two intervening fluorines is only 0.57 °K.[26] We shall therefore neglect all but the two nearest-neighbor interactions and, as will be shown, our measured spin-wave dispersion relations are consistent with this assumption.

The spin system thus may be described by the simple near-neighbor Heisenberg Hamiltonian

$$\mathcal{H} = \sum_{j>l} J_{jl}\,\vec{S}_j \cdot \vec{S}_l \,, \qquad (1)$$

$$J_{jl} = J_{AB} \text{ for nearest-neighbor } AB \text{ pair}$$

$$J_{BB} \text{ for nearest-neighbor } BB \text{ pair}$$

$$0 \quad \text{otherwise,}$$

and the only complication arises because there are six atoms per unit cell. As mentioned in Sec. I, the spin dynamics in $RbNiF_3$ have already been analyzed by Chinn *et al.*[22,27]; however, for the sake of completeness, we shall briefly outline their method. They consider the spin-raising operator

$S_l^+(t)$ on lattice site l. The lattice site is specified by the sublattice index Λ and the unit cell position $\vec{r}_n$. For a mode with wave vector $\vec{q}$ the space-time variation is of the form

$$S_l^+(t) = S_\Lambda^+ e^{i(\vec{q}\cdot\vec{r}_n - \omega t)} .$$

The six possible eigenfrequencies at each q vector are determined by the six equations of motion for spins in the unit cell, $i\dot{S}_\Lambda^+ = [S_\Lambda^+, \mathcal{H}]$, which are of the form

$$\omega S_\Lambda^+ = S_\Lambda^+ \sum_j J_{jl} S_j^z - S_\Lambda^z \sum_j J_{jl} S_j^+ . \tag{2}$$

Here the z direction is the direction of spontaneous magnetization of B spins in the hexagonal plane. We shall use the low-temperature approximation $S^z = +1$ for B-site spins and $S^z = -1$ for the A sites. The six equations of motion can be summarized as a matrix equation with the solutions for ω being the eigenvalues of the matrix $\underline{A}$:

$$A = \begin{pmatrix} J_{BB}-3J_{AB} & -J_{BB} & 0 & 0 & 0 & -J_{AB}\xi e^{iq_z c} \\ -J_{BB} & J_{BB}-3J_{AB} & 0 & 0 & -J_{AB}\xi & 0 \\ 0 & 0 & J_{BB}-3J_{AB} & -J_{BB} & -J_{AB}\zeta & 0 \\ 0 & 0 & -J_{BB} & J_{BB}-3J_{AB} & 0 & -J_{AB}\zeta \\ 0 & J_{AB}\xi^* & J_{AB}\zeta^* & 0 & 6J_{AB} & 0 \\ J_{AB}\xi^* e^{-iq_z c} & 0 & 0 & J_{AB}\zeta^* & 0 & 6J_{AB} \end{pmatrix} , \tag{3}$$

with

$$\begin{aligned} \xi &= 1 + e^{iq_x a} + \exp\left[i\left(\tfrac{1}{2}q_x a + \tfrac{1}{2}q_y \sqrt{3}\, a\right)\right], \\ \zeta &= 1 + \exp\left[i\left(\tfrac{1}{2}q_x a + \tfrac{1}{2}q_y \sqrt{3}\, a\right)\right] \\ &\quad + \exp\left[i\left(-\tfrac{1}{2}q_x a + \tfrac{1}{2}q_y \sqrt{3}\, a\right)\right], \end{aligned} \tag{4}$$

and the asterisk superscript denoting complex conjugation. As an illustration, Fig. 2 shows the eigenvalues of $\underline{A}$ in units of J_{AB} for $J_{BB}/J_{AB} = -\frac{1}{4}$ and for q along the symmetry directions ΓK, ΓM, and ΓA, where Γ, K, M, and A are the usual high-symmetry positions in the hexagonal Brillouin zone (see Fig. 3).

In Eq. (4) the components of q along ΓK, ΓM, and ΓA are q_x, q_y, and q_z, respectively. Chinn *et al.*[22] have derived analytic expressions for the magnon energies at Γ. With the notation of Fig. 2 they find

$$\begin{aligned} \Gamma_1 &= 0, \\ \Gamma_2 &= \left(J_{BB}^2 + \tfrac{9}{4}J_{AB}^2 + 9J_{AB}|J_{BB}|\right)^{1/2} + |J_{BB}| - \tfrac{3}{2}J_{AB} , \\ \Gamma_{3,4} &= 3J_{AB} , \\ \Gamma_5 &= \left(J_{BB}^2 + \tfrac{9}{4}J_{AB}^2 + 9J_{AB}|J_{BB}|\right)^{1/2} - |J_{BB}| + \tfrac{3}{2}J_{AB} , \\ \Gamma_6 &= 3J_{AB} + 2J_{BB} . \end{aligned} \tag{5}$$

The flat dispersion curves correspond to particularly simple modes in which the A spins do not move at all. In the lower mode ($\Gamma_{3,4}$ in Fig. 2) a B_2 spin moves in the exchange field of three A spins while B_1 follows B_2 in phase. B_3' moves with the same amplitude as B_2 but 180° out of phase. As is evident from Fig. 2, excitation of this mode costs an energy of $3J_{AB}$. In the upper mode (Γ_6 in Fig. 2) B_1 and B_2 are 180° out of phase, as are B_3' and B_4', so that excitation of this mode costs an additional energy of $2J_{BB}$. There is also an eigenmode in which the A spins move against stationary B spins. That occurs at the K point in the Brillouin zone and the energy is $6J_{AB}$.

IV. EXPERIMENT AND ANALYSIS

The sample was mounted in a temperature-control cryostat with the ΓA-ΓM plane horizontal. The temperature was determined by a calibrated Ge resistor at low temperatures and by a Pt thermometer at higher temperatures.

The neutron spectrometer was a conventional triple-axis instrument at the Risö DR 3 Reactor. Neutrons with wave vector $\vec{k}_i$ were extracted from

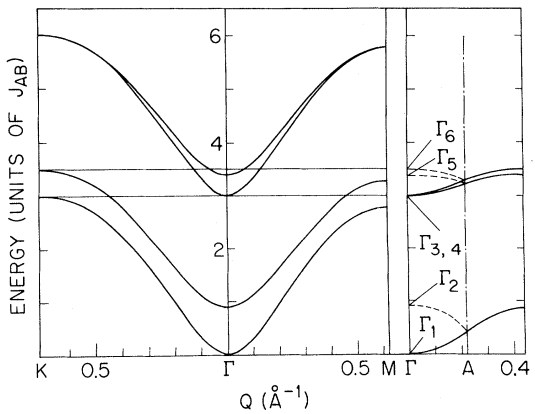

FIG. 2. Spin-wave dispersion curves in $RbNiF_3$ with the near-neighbor interactions J_{AB} and J_{BB}. The scale is relative to J_{AB} and as an illustration J_{BB} is chosen to be $-\frac{1}{4}J_{AB}$.

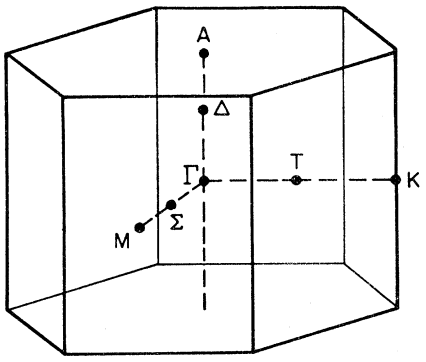

FIG. 3. Brillouin zone of a hexagonal cell with standard group-theory notation of high-symmetry points.

the reactor beam by Bragg reflection from a single-crystal monochromator. Scattered neutrons with wave vector $\vec{k}_f$ were then selected with scattering angle and subsequent Bragg reflection out from an analyzer crystal. As monochromator we used a 4-in.-high pyrolytic-graphite crystal, curved to focus the beam at the sample position.[28] The analyzer crystal was a flat pyrolytic-graphite crystal. The mosaic spread of both crystals was 0.4° full width at half-maximum (FWHM). The four collimations from reactor beam to detector were typically 36′, 40′, 35′, and 62′ FWHM.

The spectrometer was operated in the constant-$\vec{q}$ mode, that is, at fixed $\vec{q}=\vec{k}_i-\vec{k}_f-\vec{\tau}$. The intensity was measured scanning the energy transfer $\hbar\omega=(k_i^2-k_f^2)\hbar^2/2m$. The analyzer in (002) reflection was set at a fixed energy of 14 meV and the scattered beam was transmitted through a 2-in. pyrolytic-graphite filter to reduce higher-order Bragg scattering in the analyzer crystal.[29] The monochromator was used in (004) reflection for energy transfers above 20 meV. Also Zn (002) and Be (002) were used as monochromators in some scans.

The observation of spin-wave peaks in the neutron energy spectra proceeded as follows. The static magnetic-structure factor is maximal at $\vec{\tau}=(0,0,4)$, so with $(\vec{k}_i-\vec{k}_f)$ close to this lattice point we expected the acoustic spin-wave scattering to be large with a peak at an energy transfer proportional to q^2. At the bottom of Fig. 4 we show the actual neutron intensity vs $\hbar\omega$ with q at the zone boundary in the double-zone scheme or at Γ in the single-zone scheme. As q is decreased the peak position decreases, our data being shown in the lower right part of Fig. 5.

The spin-wave energy increased much more rapidly with q along ΓM, the dispersion of the acoustic spin-wave branch being shown in the lower left part of Fig. 5. This indicated that the energy of optical magnons was around 25 meV, and in the top part of Fig. 4 we show the optical spin wave at $q=0$.

The two spin-wave peaks shown in Fig. 4 are sufficient to determine the two exchange constants J_{BB} and J_{AB} ignoring further-neighbor interactions as discussed in Sec. III. With the analytic expressions [Eqs. (5)] for the $q=0$ spin-wave energies we find

$$J_{AB}=\tfrac{1}{3}\Gamma_{3,4}=8.03\pm0.2\ \text{meV}$$
$$=(93.2\pm2)\,^\circ\text{K},$$
$$|J_{BB}|=\frac{\Gamma_2^2+\Gamma_2\Gamma_{3,4}}{2\Gamma_2+4\Gamma_{3,4}}=1.82\pm0.2\ \text{meV}$$
$$=(21.1\pm2)\,^\circ\text{K}\ .$$

With these exchange constants, the full spin-wave dispersion curve along ΓM and ΓA may now

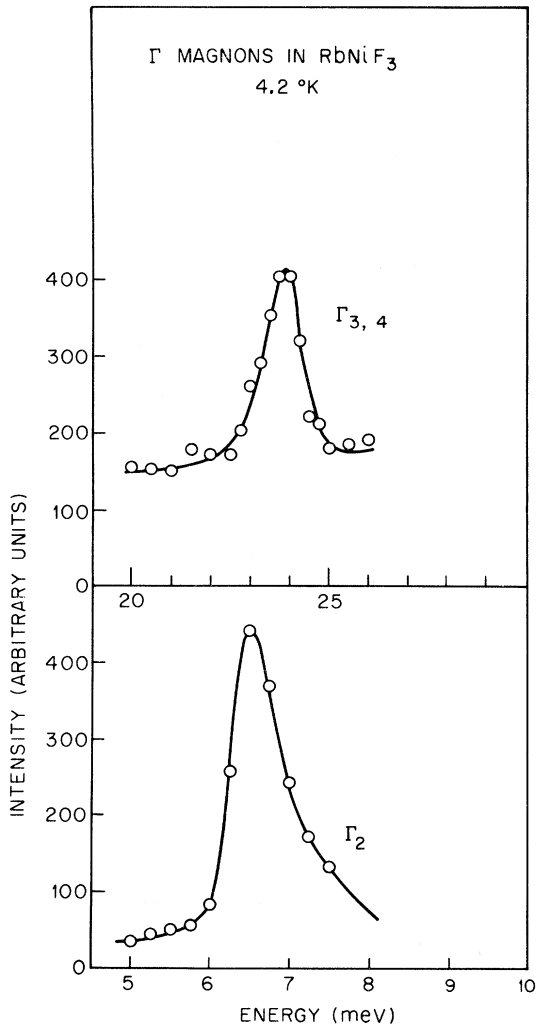

FIG. 4. Magnon peaks in the energy spectrum of scattered neutrons. Bottom: Zone-boundary acoustic magnon propagating along the c axis (double-zone scheme). Top: Optical magnon at $q=0$.

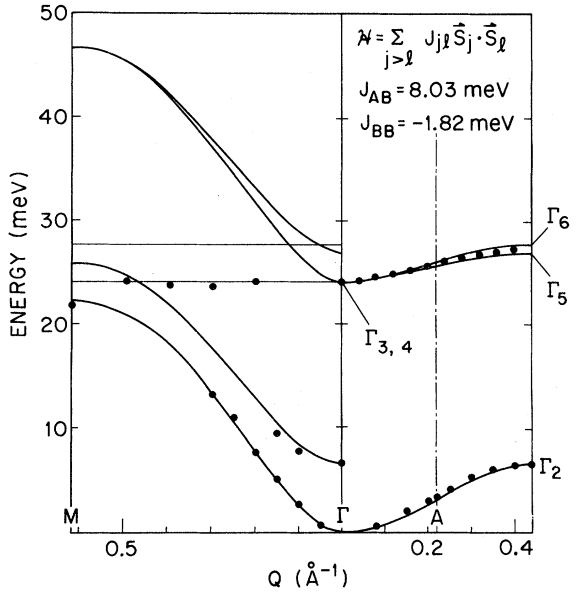

FIG. 5. Spin-wave dispersion relations in high-symmetry directions. Filled circles are the observed peak positions from data like those of Fig. 4. Full lines are calculated dispersion relations using $J_{AB} = 8.03$ meV and $J_{BB} = -1.82$ meV.

be calculated using the theory given in Sec. III; the results are the full-line curves in Fig. 5. Additional magnon peaks confirm this picture. The optical magnons along ΓA show a gentle dispersion as predicted by the spin-wave theory, although our experimental resolution is insufficient to separate the two closely lying magnons. The low-lying optical magnons along ΓM also agree well with theory. Unfortunately, the spin-wave peaks on this latter branch become broad and ill-defined for $q \gtrsim 0.15$ Å^{-1}, presumably due to magnon-phonon mixing.[30] Finally, the spin-wave energies for q along ΓM starting out from $\Gamma_{3,4}$ show no dispersion at all within the experimental resolution of 0.2 meV. Bearing in mind that in this mode the A spins are stationary, the observed lack of dispersion provides direct evidence that the second-neighbor exchange interaction within a B plane is indeed very small. However, it is not possible from our data to conclude unambiguously that all more-distant-neighbor interactions are negligible, since a fortuitous cancellation of these could in principle occur in the direction we have looked.

We have also carried out a brief survey of the energy renormalization and broadening of the spin waves as a function of temperature through T_c. Typical experimental results are shown in Figs. 6–8. Acoustic magnons propagating in the c direction (ΓA) are found to renormalize considerably, ultimately becoming overdamped at $\sim T_c$ (see Fig. 6). On the other hand, as may be seen in Figs. 7 and 8, the optical magnons at $\sim 3J_{AB}$ in both the ΓA and ΓM directions are barely affected. Distinct broadening and a slight shift in energy (~ 1 meV) occur, but the excitations remain well defined through T_c. It is important to note that for both the acoustic and optical magnons the energy renormalizations are of order J_{BB}, the important difference being that for the acoustic ΓA magnons the energy is determined primarily by J_{BB}. We shall discuss these results in more detail in Sec. V.

V. DISCUSSION—COMPARISON WITH OTHER EXPERIMENTS

A. General Comments

From the measurements and analysis of the spin-wave spectra given in Sec. IV, it is evident that the magnetic behavior of $RbNiF_3$ is quite straightforward in spite of the apparently complicated crystallographic structure. There are only two exchange constants which are of quantitative importance: J_{AB}, the exchange between A and B spins, which is strong and antiferromagnetic, and J_{BB}, the exchange between nearest-neighbor B spins, which is $4\frac{1}{2}$ times weaker and of opposite

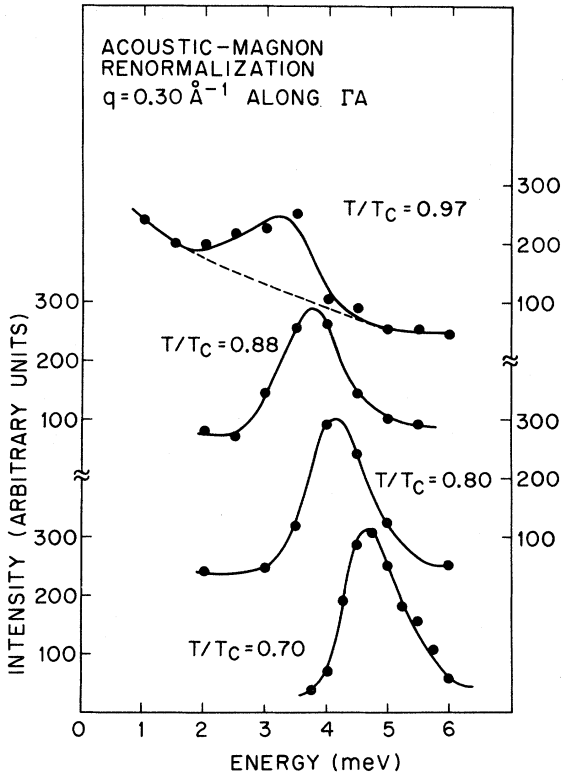

FIG. 6. Renormalization and broadening of an acoustic spin wave propagating along the c axis as the temperature is raised towards T_c.

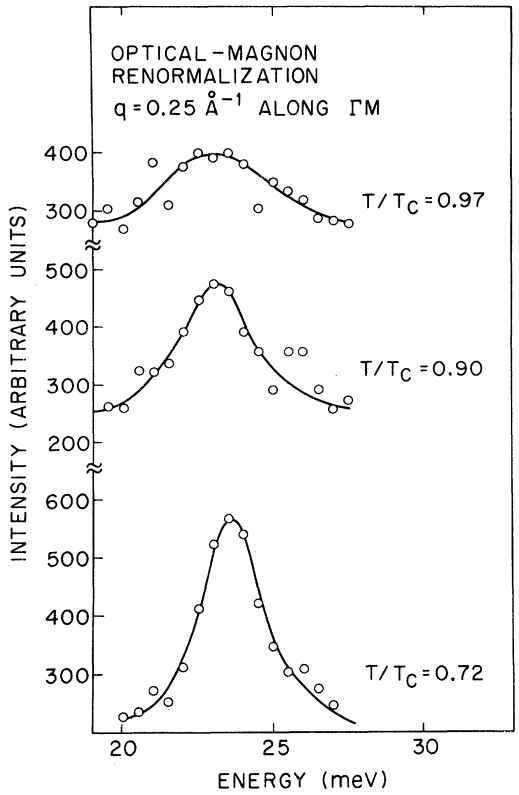

FIG. 7. Data showing the considerable broadening but very little renormalization of the flat magnons propagating along ΓM as the temperature is raised towards T_c.

sign. This difference in magnitude of J_{AB} and J_{BB} is amplified by the difference in coordination numbers, 6:1, so that the exchange field $H_{AB}(A)$ on an A atom due to the AB exchange is 27 times larger than the corresponding exchange field $H_{BB}(B)$. Thus, $RbNiF_3$ may be pictured as a set of "two-dimensional ferrimagnets" composed of three successive planes BAB, coupled internally by H_{AB}, which are then aligned relative to each other by the much smaller exchange field H_{BB}. The phase transition at 133 °K then may be viewed as a disordering of these three-plane "two-dimensional ferrimagnets" relative to each other but with the planar units remaining well correlated. One may then understand the observed temperature behavior of the spin waves rather straightforwardly. With the disassociation of the planes, energies of the order J_{BB} are lost, whereas those of order J_{AB} are maintained. Thus the acoustic magnons propagating in the c direction, which have energies fixed mainly by J_{BB}, renormalize to zero at T_c even at the zone boundary. On the other hand, the flat optical mode at $3J_{AB}$ renormalizes by less than 4% between 4.2 °K and T_c, whereas the flat optical mode at $3J_{AB} + 2|J_{BB}|$ renormalizes approximately by $2|J_{BB}|$.

The reader should be cautioned, however, that this description is extremely qualitative. We have carried out some quasielastic-scattering scans along the ΓA and ΓM directions above T_c in order to measure the wave-vector-dependent susceptibility and hence the correlation lengths within and between the hexagonal planes. These measurements are complicated by the presence of intense nuclear Bragg scattering at the reciprocal-lattice positions, so that only qualitative results could be obtained. However, it is clear from these preliminary measurements that although there is some difference in the intra- and interplanar correlation lengths, the phase transition is fully three dimensional; there is no evidence for spatial anisotropy of the sort observed, for example, in K_2NiF_4, which is a truly two-dimensional system.[31]

B. Thermodynamic Properties

In this section we shall consider experiments on a number of thermodynamic properties in the light of the microscopic exchange interactions which we have determined from the neutron-scattering experiment.

The susceptibility χ above T_c has been measured by Schafer *et al.*[12] up to temperatures of 850 °K $\sim 6.5T_c$. At high temperatures χ^{-1} approaches the asymptotic form $(T-\theta)/C$ and in the near-neighbor

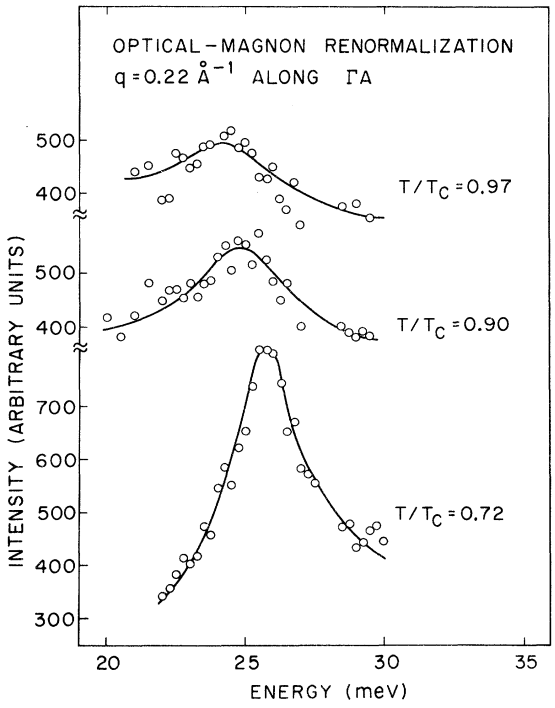

FIG. 8. Data showing that the renormalization of optical magnons propagating along the c axis mainly consists in the collapse of dispersion.

TABLE II. Exchange interactions, θ, and T_c. $\mathcal{H}=\sum_{j>l} J_{jl}\vec{S}_j\cdot\vec{S}_l$.

	J_{AB} (°K)	J_{BB} (°K)	θ^{calc} (°K)	T_c^{BPW} (°K)
Petrov *et al.* (Ref. 32)	78	0 ± 10	−211	···
Chinn *et al.* (Ref. 22)	68 ± 5	158 ± 5	−115	185
This work	93.2 ± 2.0	−21.1 ± 2.0	−239	195
θ^{expt}			−250 ± 50	
T_c^{expt}				133

model $|\theta| = \frac{2}{9}(2J_{BB}+12J_{AB})$. From about $3T_c$ the data of Schafer *et al.* show a linear variation of χ^{-1} with T with $|\theta| \simeq 250$ °K. With our values of J_{AB} and J_{BB}, we find $|\theta| = 239$ °K a satisfactory agreement. Previously reported exchange constants and the corresponding Curie-Weiss temperature are given in Table II.

The sublattice magnetizations, $\langle M_A\rangle$ and $\langle M_B\rangle$, in an applied field H_0 above T_c have been inferred from NMR experiments by Smolenskii *et al.*[16,17] The observed quantities are the line shifts for F^{19} nuclei at corner-shared and face-shared positions. In order to convert these data to sublattice magnetizations, it was necessary to assume identical hyperfine constants for F atoms in different positions; it is difficult to estimate the magnitude of the systematic error introduced by this assumption. Petrov *et al.*[32] have analyzed the sublattice magnetization in a simple mean-field cluster model taking into account only nearest-neighbor interactions. They obtain a good fit to the reported sublattice magnetizations with $J_{AB} = 78$ °K and $J_{BB} = (0 \pm 10)$ °K, values that are not very different from our results although much less accurate. Chinn *et al.*[22] have carried out calculations using a more elaborate cluster model of classical spins. Using the set of exchange constants $J_{AB} = 68$ °K, $J_{BB} = -158$ °K, and all second-neighbor interactions equal to $J^{(2)} = 5$ °K, a set which gives a completely false spin-wave spectrum, they obtain nevertheless an accurate fit with no adjustable parameters to the data of Smolenskii *et al.* We conclude therefore that the NMR experiment cannot yield unambiguous values for the exchange constants; on the other hand, our data for the exchange constants do imply sublattice magnetizations close to those observed.

The critical temperature T_c is of course also determined by the exchange interactions. It is well known that this relation is very complex, and mean-field cluster models typically overestimate T_c by as much as 35%. The cluster calculation of Chinn *et al.* gives values for the critical temperature for different exchange constants as listed in Table II as T_c^{BPW}. In view of the inherent inaccuracy of the Bethe-Peierls-Weiss method we consider the value of $T_c^{\text{BPW}} = 195$ °K with our exchange constants as reasonable. Chinn *et al.* included further-neighbor interactions and found $T_c^{\text{BPW}} = 139$ °K; we regard this small discrepancy from the actual $T_c = 133$ °K as fortuitous and it should not be considered as any indication of the magnitude of further-neighbor interactions.

C. Two-Magnon Raman Scattering

Both Fleury *et al.*[21] and Chinn *et al.*[22] have measured the Raman-scattering spectra of $RbNiF_3$ between 4.2 and ~220 °K. At 4.2 °K a broad asymmetric line is observed centered at ~510 cm^{-1} with a width of about 56 cm^{-1}. As the temperature of the sample is increased through T_c, the line shifts to lower frequency (~420 cm^{-1} at T_c) and broadens considerably, although the peak remains well defined up to at least 220 °K. From this temperature dependence both groups conclude that this feature of the scattering is magnetic in origin. Fleury *et al.* find that the peak is unaffected by magnetic fields of 50 kG, thus ruling out single-magnon excitations as the possible origin. They conclude that the scattering originates in the $\vec{S}_A\cdot\vec{S}_B$ mechanisms commonly observed in antiferromagnets.[33] This gives rise to scattering characterized by a four-spin correlation function which at low temperatures can be quantitatively explained on the basis of two strongly interacting magnons[34] with zero total wave vector created on adjacent sites. Recently Davies, Chinn, and Zeiger[35] have claimed that the temperature dependence of this peak energy can be understood on the basis of renormalized spin-wave theory up to T_c, although the energy width remains problematic.

It is of interest to reconsider the Raman-scattering results in $RbNiF_3$ in the light of our inelastic-neutron-scattering measurements. This discussion must, of course, be qualitative in nature in the absence of any detailed theory for such two-magnon scattering in this ferrimagnetic structure. As is evident from Fig. 9 the magnon density of states shows two strong peaks with a mean energy of ~26 meV and a weaker peak at ~47 meV. As discussed at the end of Sec. III the peaks in the density of states marked B, B' in Fig. 9 originate from magnons which are predominantly on the B sublattices, while the higher-energy peak arises from A-site magnons. The convoluted noninteracting two-magnon density of states for A-B magnon pairs would then exhibit a peak at $26+47=73$ meV, which is essentially the value $9J_{AB}+|J_{BB}|$ calculated by Chinn *et al.* in the noninteracting Ising approximation. Interaction effects should lower the A-B two-magnon peak by an amount of the order of J_{AB} so that from the neutron-scattering spectra we would predict that in Raman scattering one should observe a single two-magnon peak at $73-8=65$ meV $\simeq 520$ cm^{-1}. This is in good agreement with the observed value of 510 cm^{-1}.

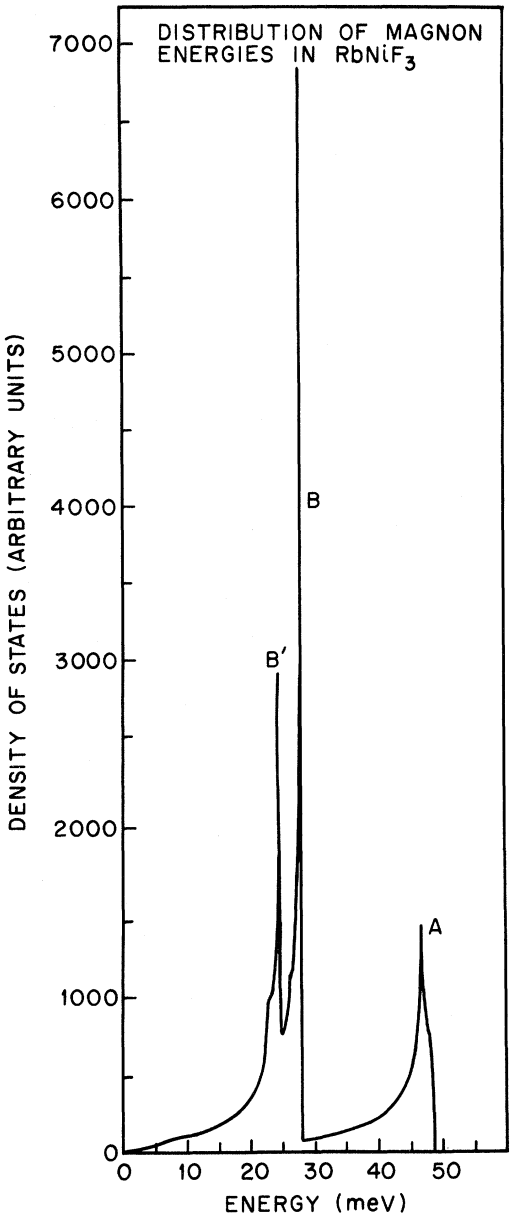

FIG. 9. Distribution of magnon energies with J_{AB} = 8.03 meV and J_{BB} = −1.82 meV. Mesh size is 0.025 meV. The two peaks B and A correspond to zone-boundary magnons with spin deviations only on the B and A sublattices, respectively.

The temperature dependence of this "four-spin-correlation-function" scattering, however, is somewhat more problematic. In the density of states the B peak collapses into the B' peak as $T \to T_c$ since the optical magnon propagating in the c direction loses its dispersion. Furthermore, the B' peak renormalizes slightly (~4%). Unfortunately, we have no direct experimental information about the A-sublattice modes at $6J_{AB}$. It seems reasonable, however, to assume that they renormalize like the mode at $3J_{AB}$, that is, by about 4%. With this assumption the net shift of the two-magnon mode would be $|J_{BB}|$(meV) + 0.04 × 73 meV = 4.7 meV = 38 cm^{-1}. This is significantly less than the observed shift of 510 − 420 cm^{-1} = 90 cm^{-1} and it indicates that the temperature dependence of the two-magnon-scattering-peak energy cannot be understood on the basis of the renormalization of the energies of the participating spin waves alone.

D. Systematics of Exchange Constants

The final result in $RbNiF_3$ which is of interest is the exchange constants themselves. Considerable effort has already been expended on first-principle calculations of covalency in an octahedral $(NiF_6)^{4-}$ complex.[36] The associated problem of Ni^{++}-F^--Ni^{++} superexchange has also received some attention,[23] although it is probably fair to say that the theory is still at the beginning stages. As noted previously, in $RbNiF_3$ one has simultaneously both 90° and 180° superexchange. The exchange constants in $RbNiF_3$ and in several other compounds are listed in Table I. In all cases the 180° exchange is strong and antiferromagnetic, as expected on the basis of Anderson's theory.[23] The 180° exchange in the oxide is approximately twice that in the fluorides, reflecting directly the increased covalent character of the oxide lattice. We note that as expected the 180° Ni^{++}-F^--Ni^{++} exchange decreases smoothly with increasing distance in going from K_2NiF_4 to $RbNiF_3$. In all cases the 90° (or near-90°) exchange is rather weaker and ferromagnetic. This is again in accordance with Anderson's ideas, although the details in this case are more complicated.[37] In particular, direct cation-cation exchange processes are probably of quantitative importance here. It is interesting to note that this 90° exchange is similar in NiO and $RbNiF_3$ in spite of the differences in anions and the geometry of the superexchange paths. Apparently, these latter two effects cancel each other.

VI. CONCLUDING REMARKS

In summary, we have carried out a detailed neutron-scattering study of the spin waves in the six-sublattice ferrimagnet $RbNiF_3$. It is found that the measured dispersion relations at 4.2 °K can be completely accounted for using simple spin-wave theory with only two exchange constants, the 180° Ni(A)-Ni(B) exchange J_{AB} = (93.2 ± 2) °K and the 90° Ni(B)-Ni(B) exchange J_{BB} = − (21.1 ± 2) °K. Using these exchange constants, other magnetic properties such as the high-temperature susceptibility, sublattice magnetization in a field, and two-magnon Raman scattering may be quantitatively understood. The actual exchange constants are

shown to be consistent with those measured in other Ni^{++} insulators with octahedral anion coordination. A calculation of the 90° and 180° exchange constants in $RbNiF_3$ offers an important challenge to the theorist.

The temperature behavior of the spin waves in $RbNiF_3$ is of particular note. As the temperature is raised towards T_c, the acoustic magnons propagating along the c direction renormalize to zero like the magnetization. On the other hand, the optical magnons at $3J_{AB}$ barely renormalize at all. This is consistent with the physical picture in which $RbNiF_3$ is viewed as a set of two-dimensional ferrimagnets composed of three successive Ni^{++} planes *BAB*. These *BAB* units are then coupled to each other by the weaker exchange field H_{BB}. Thus at the phase transition only energies of the order of J_{BB} are lost to the excitations.

ACKNOWLEDGMENT

We should like to thank S. R. Chinn for stimulating our interest in this compound and for a number of helpful conversations.

[1]A. Okazaki, K. C. Turberfield, and R. W. H. Stevenson, Phys. Letters 8, 9 (1964); O. Nikotin, P. A. Lindgard, and O. W. Dietrich, J. Phys. C 2, 1168 (1969).

[2]C. G. Windsor and R. W. H. Stevenson, Proc. Phys. Soc. (London) 87, 501 (1966).

[3]R. A. Cowley, P. Martel, and R. W. H. Stevenson, Phys. Rev. Letters 18, 162 (1967).

[4]J. Skalyo, Jr., G. Shirane, R. J. Birgeneau, and H. J. Guggenheim, Phys. Rev. Letters 23, 1394 (1969).

[5]M. T. Hutchings and E. J. Samuelsen, Solid State Commun. 9, 1011 (1971).

[6]E. J. Samuelsen, R. Silberglitt, G. Shirane, and J. P. Remeika, Phys. Rev. B 3, 157 (1971).

[7]L. Passell, O. W. Dietrich, and J. Als-Nielsen, in *Proceedings of the Fifteenth Annual Conference on Magnetism and Magnetic Materials, Chicago*, 1971, *No.* 5, edited by C. D. Graham, Jr. and J. J. Rhyne (AIP, New York, 1971), p. 1251.

[8]T. Riste, J. Phys. Soc. Japan Suppl. B-III 17, 60 (1962).

[9]B. N. Brockhouse and H. Watanabe, in *Inelastic Scattering of Neutrons in Solids and Liquids* (IAEA, Vienna, 1963), Vol. II, p. 207.

[10]W. Rüdorff, J. Kändler, and D. Babel, Z. Anorg. Allgem. Chem. 317, 261 (1962).

[11]G. A. Smolenskii, V. M. Yudin, P. P. Syrnikov, and A. B. Sherman, Fiz. Tverd. Tela 8, 2965 (1966) [Sov. Phys. Solid State 8, 2368 (1967)].

[12]M. W. Schafer, T. R. McGuire, B. E. Argyle, and G. J. Fan, Appl. Phys. Letters 10, 202 (1967).

[13]S. J. Pickart and H. A. Alperin, J. Appl. Phys. 42, 1617 (1971).

[14]J. E. Weidenborner and A. L. Bednowitz, Acta Cryst. B 26, 1464 (1970).

[15]E. I. Golovenchits, A. G. Gurevich, and V. A. Sanina, Zh. Eksperim. i Teor. Fiz. Pis'ma v Redaktsiyu 3, 408 (1966) [Sov. Phys. JETP Letters 3, 266 (1966)].

[16]G. A. Smolenskii, R. V. Pisarev, M. P. Petrov, V. V. Moskalev, I. G. Siny, and V. M. Judin, J. Appl. Phys. 39, 568 (1968).

[17]G. A. Smolenskii, M. P. Petrov, V. V. Moskalev, V. S. L'vov, V. S. Kasperovich, and E. V. Zhironova, Fiz. Tverd. Tela 10, 1305 (1968) [Sov. Phys. Solid State 10, 1040 (1968)].

[18]G. Zanmarchi and P. F. Bongers, Solid State Commun. 6, 27 (1968).

[19]J. Tylicki, W. M. Yen, J. P. van der Ziel, and H. J. Guggenheim, Phys. Rev. 187, 758 (1969).

[20]S. R. Chinn and H. J. Zeiger, Phys. Rev. Letters 21, 1589 (1969).

[21]P. A. Fleury, J. M. Worlock, and H. J. Guggenheim, Phys. Rev. 185, 738 (1969).

[22]S. R. Chinn, H. J. Zeiger, and J. R. O'Connor, Phys. Rev. B 3, 1709 (1971).

[23]P. W. Anderson, in *Solid State Physics*, edited by F. Seitz and D. Turnbull (Academic, New York, 1963), Vol. 14, p. 99.

[24]J. Owen and J. H. M. Thornley, Rept. Progr. Phys. 29, 675 (1966).

[25]H. Guggenheim, J. Appl. Phys. 34, 2482 (1963).

[26]Y. Yamaguchi, J. Phys. Soc. Japan 29, 1163 (1970).

[27]For a more complete discussion of the theory, see S. R. Chinn, Ph.D. thesis (M.I.T., 1970) (unpublished).

[28]T. Riste, Nucl. Instr. Methods 86, 1 (1970); A. C. Nunes and G. Shirane, *ibid.* 95, 445 (1971).

[29]B. O. Loopstra, Nucl. Instr. Methods 44, 181 (1966); G. Shirane and V. J. Minkiewicz, *ibid.* 89, 109 (1970).

[30]There are in all 90 branches in the phonon spectrum; most of the Raman-active modes have been identified by Fluery *et al.* (Ref. 21).

[31]R. J. Birgeneau, H. J. Guggenheim, and G. Shirane, Phys. Rev. Letters 22, 720 (1969); R. J. Birgeneau, J. Skalyo, Jr., and G. Shirane, Phys. Rev. B 3, 1736 (1971).

[32]M. P. Petrov, V. V. Moskaley, and V. S. Kasperovich, Fiz. Tverd. Tela 12, 2063 (1970) [Sov. Phys. Solid State 12, 1637 (1971)].

[33]P. A. Fleury and R. Loudon, Phys. Rev. 166, 514 (1968).

[34]R. J. Elliott, M. F. Thorpe, G. F. Imbusch, R. Loudon, and J. B. Parkinson, Phys. Rev. Letters 21, 147 (1968).

[35]R. W. Davies, S. R. Chinn, and H. J. Zeiger, Phys. Rev. B 4, 992 (1971).

[36]D. E. Ellis, A. J. Freeman, and P. Ros, Phys. Rev. 176, 688 (1968).

[37]N. L. Huang, Phys. Rev. 157, 378 (1968).